ACES Asian Chemical Editorial Society

DOI: 10.1002/asia.201801421

CHEMISTRY AN ASIAN JOURNAL Full Paper

Self-Assembly

Supramolecular Chiral Helical Ribbons of Tetraphenylethylene-Appended Naphthalenediimide Controlled by Solvent and Induced by L- and D-Alanine Spacers

Santosh P. Goskulwad,[a, b] Mohammad Al Kobaisi,[c] Duong Duc La,[d] Rajesh S. Bhosale,[a, g] Malavath Ratanlal,[e] Sidhanath V. Bhosale,*[a, b] and Sheshanath V. Bhosale*[f]

Abstract: Naphthalenediimide-tetraphenylethylene conjugates with an alanine spacer (coded as: **NDI-(Ala-TPE)$_2$**) were synthesized to study the influence of the chirality of the amino acid spacer on its self-assemblies. Here we particularly show that NDI-Ala-TPE bearing L-alanine gives left-handed (M-type) helical superstructure, while D-alanine produces right-handed (P-type) helical ribbons in THF:H_2O at 40:60% v/v ratio. However, particular aggregates were observed at 20:80% v/v ratio. Circular dichroism was used to characterise the induction of chirality and the handedness of the helical superstructures, and the microstructure of the self-assembled materials was visualised using scanning electron microscopy while DLS analysis confirmed the formation of particular aggregates in solution.

Introduction

Tetraphenylethylene (TPE) and its derivatives have been widely used as an AIE-active luminogens especially in the designing of mechanochromic luminescent materials, due to their non-emissive behaviour in dilute solution and highly emissive upon aggregation/self-assembly and solid state in phenomenon called aggregation induced emission (AIE).[1] Nevertheless, TPE derivatives also used in biological science and technological development such as chemosensors, biomarkers, cell labelling, lasing materials, OLED and solar cell applications.[2] Taking advantages of AIE activity of TPE, its derivatives widely used as supramolecular building blocks for the construction of various nanostructures (nano-rings, capsules, flowers, nanofibres, bird nests etc.).[3] Literature search revealed that there are only few reports about the fabrication of helical materials via supramolecular self-assembly of TPE derivatives. The helical self-assembled materials were achieved by incorporating chiral centre in the building blocks.[4] The chiral supramolecular self-assembled material could also be obtained through self-assembly of achiral building blocks such as TPE bearing long alkyl chains with amide linkage.[5] Such TPE derivatives produce chiral helical self-assembly, where helicity was controlled by the odd/even effect of the linking carbon chains, typically, even carbon chains produce right-handed and odd carbon chains produce left handed helical superstructures.[6]

In the last two decades, naphthalenediimide (NDI) and its derivatives gained researchers attention due to their applicability in various field such as supramolecular, medicinal, and organic electronics.[7] NDI can be functionalised through both the imide positions as well as the four aromatic positions of the core,[8] to give materials with potential applications as n-type semiconductors, field effect transistors, artificial photosynthesis, fluorescence emitters, biosensors as well as formation of various self-assembled nano-structures.[9] Recently, we functionalised NDIs with TPE on to the core positions to convert NDIs from aggregation-caused quenching (ACQ) active to AIE active materials.[1,10] To this, we have synthesised NDI bearing

[a] S. P. Goskulwad, Dr. R. S. Bhosale, Dr. S. V. Bhosale
Polymers and Functional Materials Division
CSIR-Indian Institute of Chemical Technology
Hyderabad 500007, Telangana (India)
E-mail: bhosale@iict.res.in

[b] S. P. Goskulwad, Dr. S. V. Bhosale
Academy of Scientific and Innovative Research (AcSIR)
Ghaziabad-201002 (India)

[c] Dr. M. A. Kobaisi
School of Science, Faculty of Science, Engineering and Technology
Swinburne University of Technology
Hawthorn (Australia)

[d] Dr. D. D. La
Institute of Chemistry and Materials
Hoang Sam, Hanoi (Vietnam)

[e] M. Ratanlal
Organic Synthesis and Process Chemistry Division
CSIR-Indian Institute of Chemical Technology
Hyderabad 500007, Telangana (India)

[f] Prof. S. V. Bhosale
Department of Chemistry
Goa University
Taleigao Plateau, Goa-403 206 (India)
E-mail: svbhosale@unigoa.ac.in

[g] Dr. R. S. Bhosale
Present Address:
Department of Chemistry
Indrashil University
Kadi, Mehsana, 382740 (India)

Supporting information and the ORCID identification number(s) for the author(s) of this article can be found under:
https://doi.org/10.1002/asia.201801421.

one, two or four TPE moieties on to the core and studied their optical, fluorescence and self-assembled various nanostructures in mixtures of polar-nonpolar solvents, and aggregated species producing high quantum yield such as 9, 18 and 21%, respectively.[10] Although, core functionalised NDI through core-substitution produced high quantum yields, other examples of N- functionalised perylenediimides (PDIs) with TPE also exhibit desirable quantum efficiency.[10,11]

Mimicking biological systems in material fabrication of supramolecular self-assembled materials is achieved via designing molecular functionalities[12] allowing for non-covalent interactions such as hydrophobic, van der Waals, hydrogen bonding, electrostatic and π–π stacking.[12c–e] However, to construct controlled nanostructures through supramolecular chemistry mechanistic study is a need.[14] In recent years, following these principals in molecular design, such building blocks are employed to self-assemble into helical functional materails with controlled nanometer scale dimentions.[13] Among these building blocks amino acids and peptides are of a special importance due to these inherent chiral centres to fabricate supramolecular helical structures.[13,14]

Herein, we designed and synthesised NDI bearing TPE functionality to diimide positions with L- or D-alanine as a spacer to investigate three important aspects; (1) whether TPE functionalised NDI induces AIE activity upon aggregation, (2) the effect of Restriction of Intramolecular Rotation (RIR) mechanism on self-assembly, and (3) whether chiral spacer can induce chirality in self-assembled nanostructures. Typically, NDI bearing TPE moieties with L- and D-alanine spacers were synthesised in two steps: first, the preparation of L-Ala-TPE (Scheme 1), followed by condensation of naphthalene dianhydride with L- or D-Ala-TPE, giving 60% of **NDI-(L-Ala-TPE)$_2$** and 58% of **NDI-(D-Ala-TPE)$_2$**, respectively (Scheme 2. Furthermore, the self-assembly behaviour of both derivatives were monitored by UV-vis

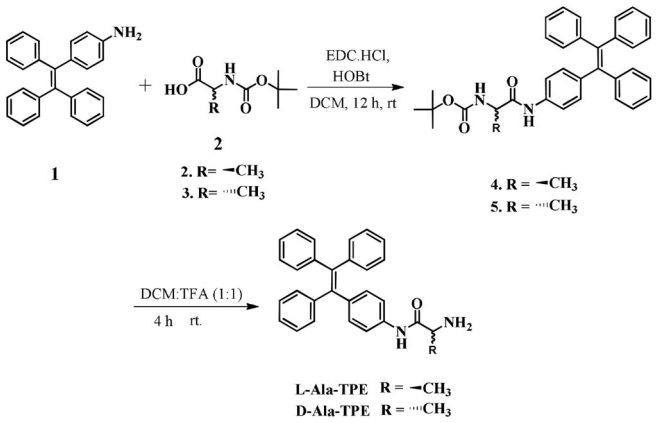

Scheme 1. Synthetic pathway of L-**Ala-TPE** and **D-Ala-TPE**.

absorption and fluorescence emission and circular dichroism (CD) spectroscopy, and supramolecular structures were imagined using field emission scanning electron microscopy (SEM) and polarized optical microscopy.

Results and Discussion

UV-vis absorption spectroscopy used to evaluate the solvent role in the self-assembly process. **NDI-(L-Ala-TPE)$_2$** in THF gives three typical absorption band at 345, 352 and 375 nm (Figure 1). Furthermore, Figure 1b shows the UV-vis absorption changes of **NDI-(L-Ala-TPE)$_2$** in THF with varying water ratios. Upon incremental the percentage of water content of **NDI-(L-Ala-TPE)$_2$** solution in THF, the absorption peaks increase with bathochromic shift band to 385 nm. Upon addition of 90% water in THF the absorption band (blue in color) broaden with 15 nm red-shift to 395 nm. Similar trend was also observed for NDI bearing D-alanine (Figure S1a). These results clearly dem-

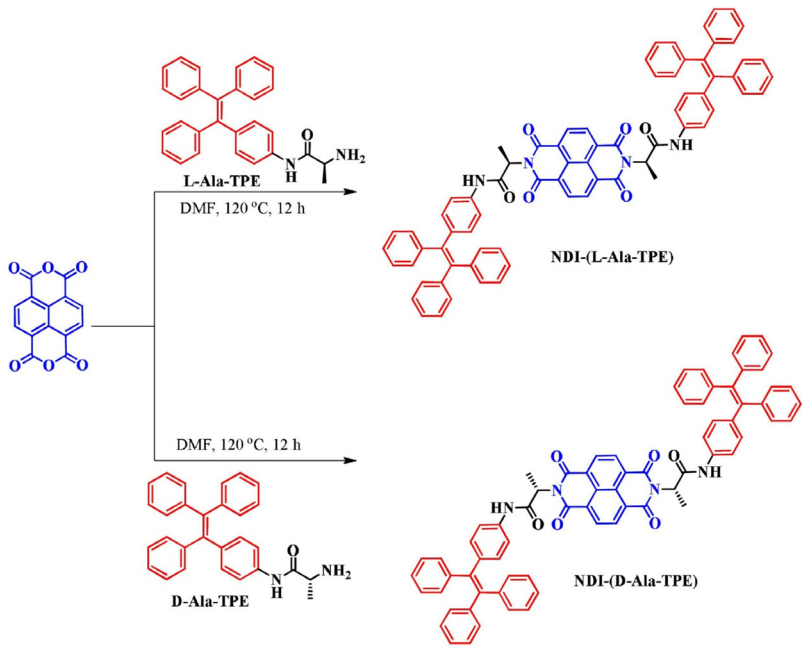

Scheme 2. Synthetic pathway of **NDI-(L-Ala-TPE)$_2$**and **NDI-(D-Ala-TPE)$_2$**.

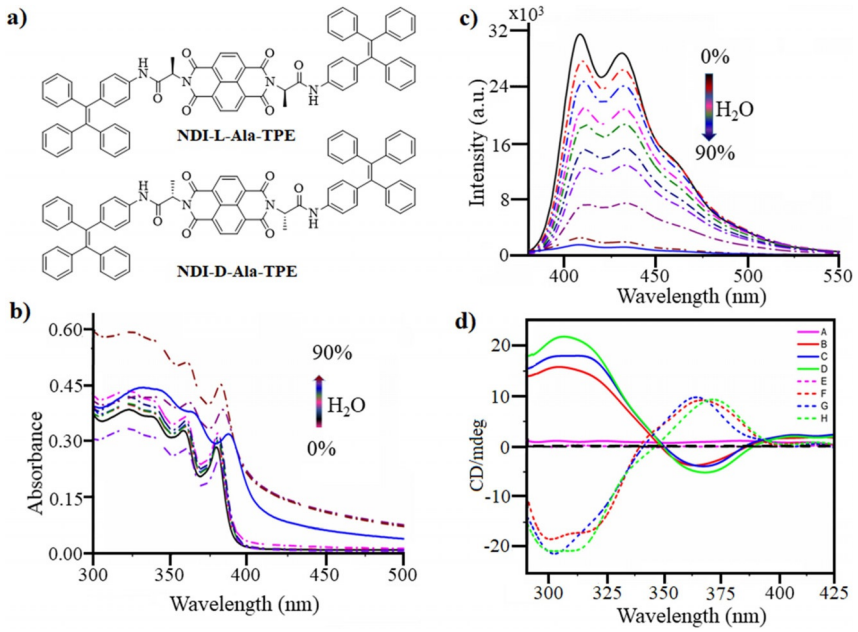

Figure 1. (a) Structures of **NDI-(L-Ala-TPE)$_2$** and **NDI-L-Ala-TPE** used in this study. (b&c) UV-vis spectra and (b) Fluorescence emission spectra of **NDI-(L-Ala-TPE)$_2$** (1×10^{-5} M) in THF and increasing water ratios (0–90%). (d) Circular Dichroism (CD) of **NDI-(L-Ala-TPE)$_2$** (dotted line) and **NDI-(D-Ala-TPE)$_2$** (solid line) with conc. 1×10^{-5} M in THF/water *v/v* ratios: A, E (in THF) and B, F (10:90); C, G (20:80%) and D, H (40:60).

onstrate NDI bearing TPE with alanine spacer shows *J*-type aggregation in THF/water mixes because of strong π–π stacking interactions of NDI core. Furthermore, fluorescence (FL) spectroscopy used to demonstrate mode of aggregation in various THF/water mixture for both the derivatives **NDI-(L-Ala-TPE)$_2$** (Figure 1c) and **NDI-(D-Ala-TPE)$_2$** (Figure S1b). Figure 1c shows the fluorescence of **NDI-(L-Ala-TPE)$_2$** in THF with strong peaks at 410 and 438 nm ($\lambda_{ex}=375$ nm) and quantum yield of 4.3%, however, FL intensity decreases upon increasing the water ratio in THF. Exactly, similar trend was observed in the case of **NDI-(D-Ala-TPE)$_2$** as shown in Figure S1b. These results clearly demonstrate the effect of solvent polarity on self-assembly and molecular aggregation. The decrease in emission peak intensity indicated strong π–π stacking of NDI cores leading to *J*-type aggregation.

Recently, Zhang et al. proposed mechanism for fluorescence quenching of TPE-PBI derivatives with TPE substitution at imide position.[15] Herein, we propose similar mechanism for emission behaviour of **NDI-(L-Ala-TPE)$_2$** and **NDI-(D-Ala-TPE)$_2$** in THF:water. Our group studied the AIE behaviour of TPE-NDI with TPE at core of NDI. TPE substitutions at the core of NDI restricted the π–π-stacking with planar conformation of the NDI core, which causes enhanced fluorescence emission.[10b] Whereas, the TPE-substitution at imide of NDI exhibits aggregation-caused quenching (ACQ) emission. For **NDI-(L-Ala-TPE)$_2$** and **NDI-(D-Ala-TPE)$_2$** in THF:water ($f_w=90$%), the emission peak is completely quenched upon aggregation. The fluorescence emission quenching may be arise due to *J*-aggregation state due to π–π staking interactions between NDI cores. The RIR mechanism of the AIE process indicates in solution TPE is non-emissive. Chromophores **NDI-(L-Ala-TPE)$_2$** and **NDI-(D-Ala-TPE)$_2$** are non-fluorescent in solution state upon excitation of TPE subunit. Furthermore, in aggregate state the RIR process brings fluorescence quenching of the dyads. The fluorescence emission quenching phenomenon is ascribed to photo-induced charge transfer (PICT) between TPE and NDI though TPE is not strong electron donor and NDI is very good acceptor.

CD spectroscopy was used to determine whether spacer alanine induces chirality in the self-assembled supramolecular structures. Figure 1d, clearly shows a significant Cotton effect upon increasing the water ratio in THF/water solutions of both stereoisomers **NDI-(L-Ala-TPE)$_2$** (dotted line) and **NDI-(D-Ala-TPE)$_2$** (solid line) with exactly opposite handedness. CD spectra give a isodichroic point at 348 nm zero crossing. Pure THF solutions of both stereoisomers were CD inactive (Figure 1d, curve A and E), as expected, CD activity increases with increasing water ratio due to increasing molecular self-assembly. Typically, **NDI-(L-Ala-TPE)$_2$** in THF/water ($f_{T/W}$ 40:60 *v/v*) solution, shows significant a bisignate CD signals observed in both the TPE and NDI absorption region, that is, negative at 310 nm and positive at 362 nm, which is characteristic of excitonically-coupled helical organization of the **NDI-(L-Ala-TPE)$_2$** chromophores. In THF/water ($f_{T/W}$ 10:90 *v/v*) **NDI-(L-Ala-TPE)$_2$** gives similar handed chiral CD spectrum, with decreasing peaks intensity, this can be due to increase in the amorphous nature of aggregates at this high ratio of poor solvent. Completely opposite bisignate CD signals observed in the case of **NDI-(D-Ala-TPE)$_2$**, that is, +ve at 310 nm and -ve at 362 nm (Figure 1d).

Dynamic light scattering (DLS) measurements were performed on **NDI-(L-Ala-TPE)$_2$** and **NDI-(D-Ala-TPE)$_2$** in various ratios of THF/water. The DLS of **NDI-(L-Ala-TPE)$_2$** gives size distributions with average size of 614 nm in $f_{T/W}$ 40:60, *v/v*. When increase percentage of the water in THF, a prominent peak ap-

peared at 254 nm in $f_{T/W}$ 20:80 *v/v* and 268 nm in $f_{T/W}$ 10:90 *v/v*, as shown in ESI Figure S2. Similar DLS trend was observed for **NDI-(D-Ala-TPE)$_2$**, showing that the diameter of aggregate structures is about 224 nm in $f_{T/W}$ 10:90, *v/v*, whereas 275 nm in $f_{T/W}$ 20:80, *v/v*, and about 716 nm in $f_{T/W}$ 40:60, *v/v* (Figure S3). DLS analysis clearly suggested directional growth increases up to $f_{T/W}$ about 40:60, while a different nucleation based mechanism of aggregation appears up on increasing the poor solvent water ratio beyond this optimum resulting in smaller particulate aggregates for both stereoisomers.

To evaluate the mode of aggregation and nanostructures assembly, SEM was used to image microstructures deposited after solvent evaporation. **NDI-(L-Ala-TPE)$_2$** and **NDI-(D-Ala-TPE)$_2$** microstructures were tuned under solvophobic effects of good solvent (THF) and a poor solvent (water) mixture. Mixtures of THF/water with high water volumetric ratios above 80% produced nano-spheres for both stereoisomers. Nevertheless, both the derivatives produce helical ribbons with 60% water content in THF (Figure 2, Figure S4). The twisted ribbons obtained for both **NDI-(L-Ala-TPE)$_2$** and **NDI-(D-Ala-TPE)$_2$** from

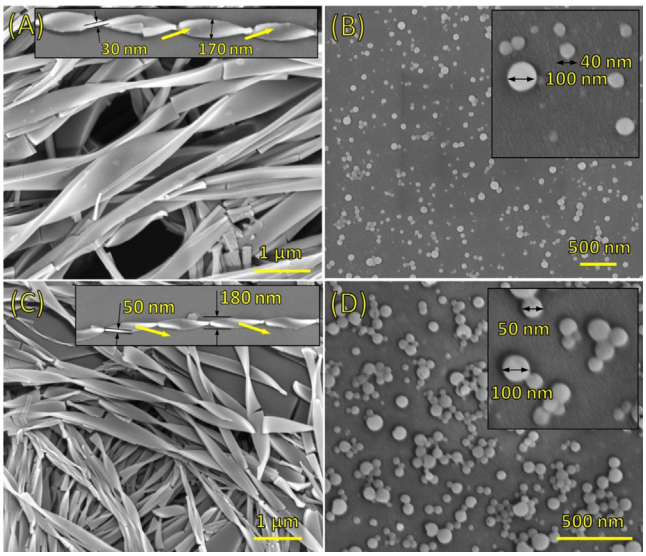

Figure 2. SEM images of **NDI-(L-Ala-TPE)$_2$** and **NDI-(D-Ala-TPE)$_2$** deposited from solutions in THF:H_2O at 40:60 *v/v* (A&C) and 20:80 *v/v* ratios (B&D), respectively.

$f_{T/W}$ 40:60 were below 1 μm in width and below 100 nm in thickness. Nevertheless, **NDI-(L-Ala-TPE)$_2$** and **NDI-(D-Ala-TPE)$_2$** produced twisted ribbons with opposite directions giving unexpected M-type and P-type helicity, respectively (see Figure 2A and 2C). The self-assembly of both stereoisomers resulted in preferentially well-defined tens of micrometres in length M- and P-type twisted ribbons. The SEM images in Figure 2A (inset) shows a typical long twisted ribbon approximately 170 nm wide, 30–50 nm in thickness and twist half period in the range of ≈350 nm. In some instances, the ribbon structures hierarchically accumulate to form larger ribbon, and in some occasions the twisted ribbons have completely unwound resulting in flat ribbon adhering to the silicon wafer substrate surface. Literature search revealed that L and D-alanine derivatives, LPA and DPA, in polar solvents such as acetonitrile yield unexpected M and P-types of helical ribbons, respectively.[16]

Our findings of helical superstructure with opposite preferential well agreement with the results reported by Wang et al. in polar solvents.[15] Figure 2B and D show 10–100 nm in diameter microspheres were obtained from both stereoisomers in the $f_{T/W}$ 20:80 *v/v* ratio. We believe that increasing poor solvent that is, water content intensifies the solvophobic interactions, limiting the directional growth during solvent evaporation, and promoting the growth around the initial nucleation centres resulting in spherical aggregates.

Optical microscopy also supports similar trend of self-assembly, fibril structure in $f_{T/W}$ 40:60 *v/v* (Figure S5A and Figure S5C) and particular aggregates in $f_{T/W}$ 20:80 *v/v* ratios were observed (ESI Figure S5B and Figure S5D). SEM and optical images are in good agreement with DLS analysis (Figure S2 and S2). The crystalline properties of **NDI-(L-Ala-TPE)$_2$** and **NDI-(D-Ala-TPE)$_2$** monomer and self-assembly in THF/H_2O mixture was investigated by XRD patterns (Figure S6). It can be seen that **NDI-(L-Ala-TPE)$_2$** and **NDI-(D-Ala-TPE)$_2$** are amorphous solid in the monomer form. However, after self-assembly in THF/H_2O, **NDI-(L-Ala-TPE)$_2$** and **NDI-(D-Ala-TPE)$_2$** aggregates become crystalline in nature as the presence of strong diffraction peaks in XRD patterns. The positions and shape of diffraction peaks are in good agreement with the structures observed in SEM and POM images.

Further, investigating the electronic structure and transitions of **NDI-(L-Ala-TPE)$_2$** and **NDI-(D-Ala-TPE)$_2$** shows identical electronic structures and transition energies. Time dependent density functional theory (TDDFT) calculations were carried out in vacuo using Gaussian 16 suit of programs and the B3LYP/6-31G(d,p)//B3LYP/6-311+G(d,p) level of theory.[17] The in vacuo TDDFT results were processed using Gauss-Sum 3.0 program[18] to calculate the group contributions to the HOMO and LUMO orbitals and simulate the density of states (DOS) (Figure S7A), UV-vis (Figure S7B) and CD spectra (Figure S8A and Figure S8B) of **NDI-(L-Ala-TPE)$_2$** and **NDI-(D-Ala-TPE)$_2$**. The DOS and CD spectra are produced by convoluting the molecular orbital and transitions information obtained from the Gaussian modelling results. The pair stereoisomers gave a HOMO that is concentrated on one of the TPE moieties, and a LUMO that is concentrated on the NDI acceptor core of the **NDI-(L-Ala-TPE)$_2$** and **NDI-(D-Ala-TPE)$_2$** (See Figure 3). Very low oscillation strength (f) associated with HOMO→LUMO spectroscopic excitation was obtained which is in agreement with measurement. The HOMO—LUMO gap as per simulated DOS spectra of **NDI-(L-Ala-TPE)$_2$** and **NDI-(D-Ala-TPE)$_2$** is identical, 1.79 eV (See Figure S7a). Although the electronic structure and electronic transitions are identical for **NDI-(L-Ala-TPE)$_2$** and **NDI-(D-Ala-TPE)$_2$**, the simulated CD spectra show opposite signals (See Figure S8A and Figure S8B) for the two stereoisomers as expected in agreement with experimental results (see Figure 1d).

The self-assembly of **NDI-(L-Ala-TPE)$_2$** and **NDI-(D-Ala-TPE)$_2$** is driven by solvophobic effect at higher water volumetric ratio of 40:60 *v/v* ratio of THF/water solvent mixture. Both stereoisomers stack via the planar NDI core driven by the quadrupole

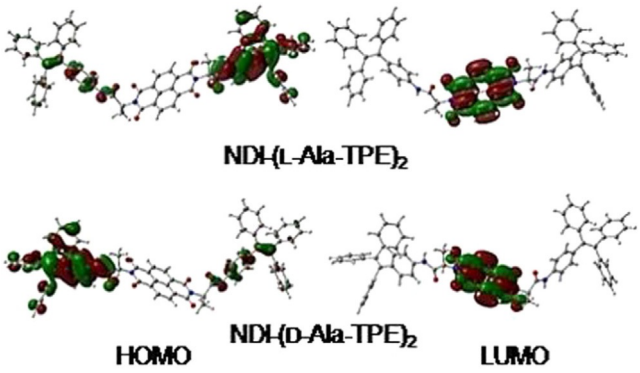

Figure 3. Schematic representation of the self-assembly of **NDI-(L-Ala-TPE)$_2$** (left) and **NDI-(D-Ala-TPE)$_2$** (right) to from helical ribbon and nanoparticles as a function of solvophobic effect when tuned by THF water ratio.

moment interaction between the π electron densities preferentially through off centre face to face parallel stacking. But due to the large size of the hydrophobic aromatic TPE moieties an in-plane twisted is introduced, which amplifies in the z-direction, resulting in a helical assembly.

The chiral centres of the L- or D-Ala linking the NDI core to the two TPE moieties determines the direction of the in-plane twisted of stacked molecules, resulting in supramolecular chirality producing M (left-handed) and P (right-handed) type helicity, respectively (see Figure 4). Increasing the water ratio to 20:80 *v/v* THF/water did not allow for directional growth in the z-direction, instead the aggregation starts with micellar nuclei that grow by adding layers positioning the more hydrophilic parts of the molecule towards the aqueous solvent environment as shown in Figure 4. The chirality of the spherical superstructure is produced due to the same in-plane angular twists between molecules in the concentric stacked layers directed by the L- or D-Ala chiral centres.

Conclusions

In summary, we report the synthesis of TPE-appended NDI using L- and D-alanine spacers (**NDI-(L-Ala-TPE)$_2$** and **NDI-(D-Ala-TPE)$_2$**) and the formation of chiral supramolecular twisted ribbons based on solvophobic control. The amino acid induced self-assembly to give left- and right-handed microarchitectures, respectively. These results demonstrate that a small spacer can induce chirality in the supramolecular structures and that the assembly can be controlled by the proportion of used solvents. The reported supramolecular chiral system is particularly interesting, since it is based on a n-type NDI core and may offer practical value, such as templates for helical crystallisation and materials for optoelectronic devices.

Experimental Section

Materials

All reactions were performed under inert atmosphere. All the chemicals were purchased from Sigma–Aldrich, Bangalore, Karnataka, India and used without purification. Solvents were dried by standard methods to use for reactions. TLC was carried out with Merck silica gel 60-F254 plates and column chromatography was performed over silica gel (60–120 mesh) obtained from commercial suppliers. ^{1}H NMR and ^{13}C NMR spectra were recorded on a Bruker spectrometer using $CDCl_3$, [D6]DMSOas solvent and tetramethylsilane as an internal standard. Mass and HRMS spectrometric data were recorded by electron spray ionization (ESI) technique.

Sample preparation: A 0.2 mL of stock solution of **NDI-(L-Ala-TPE)$_2$** and **NDI-(D-Ala-TPE)$_2$** (10^{-4} M) was injected into 2 mL of THF/water with various ratios in different volumetric flasks and solution allowed to equilibirate for additional 1 h prior to measurements.

Scanning Electron Microscopy (SEM): The cleaned silicon wafer used for SEM measurements, firstly sample droped on silicon wafer upon solvent evaporation and then sputter coated with gold for 10 s at 0.016 mA Ar plasma (SPI, West Chester, USA) for SEM imag-

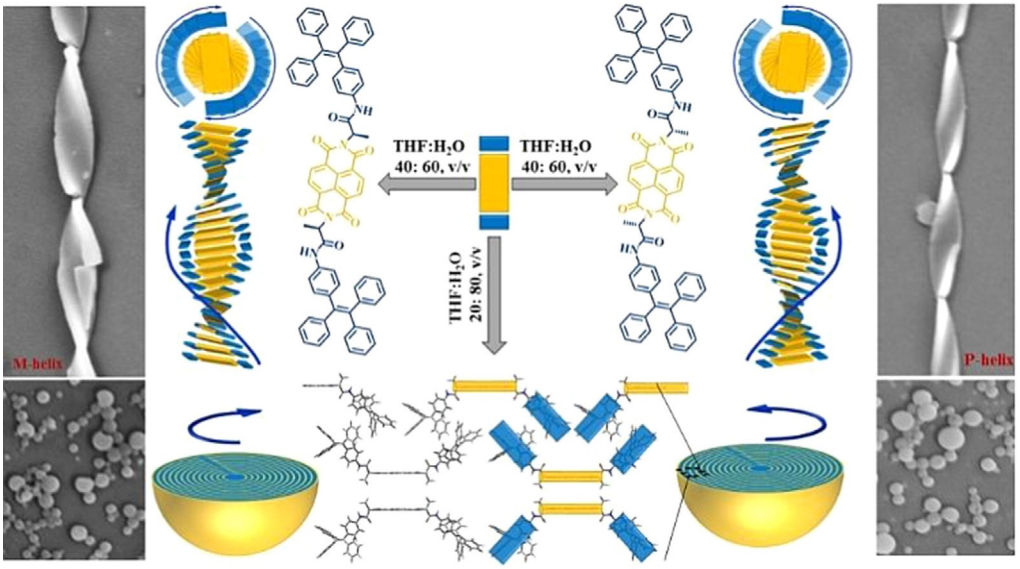

Figure 4. Schematic representation of the self-assembly of **NDI-(L-Ala-TPE)$_2$** (left) and **NDI-(D-Ala-TPE)$_2$** (right) to from helical ribbon and nanoparticles as a function of solvophobic effect when tuned by THF water ratio.

ing using a FEI Nova NanoSEM (Hillsboro, USA) operating at high vacuum at the voltage of 15 keV.

TEM imaging: Similr to SEM, TEM images were collected upon solvent evaporation on a holey carbon coated copper grid and micrographs were recorded with a JEOL 1010 100 kV transmission electron microscope.

Circular dichroism: CD spectra were recorded with an AVIV 202 CD spectrometer under a nitrogen atmosphere. Experiments were performed in a quartz cell with 1 mm path length in the range of 275–425 nm at room temperature.

Synthesis of Intermediates

Synthesis of Compound 4

To a solution of N-(tert-butoxycarbonyl)-L-alanine **2** (100 mg, 0.52 mmol) in 5 mL dry dichloromethane, EDC.HCl (120 mg, 0.62 mmol) and HOBt (95 mg, 0.62 mmol) were added. The reaction mixture was stirred at room temperature under nitrogen for 30 minutes. The 4-(1,2,2-triphenylvinyl)aniline**1** (184 mg, 0.52 mmol) was then added to reaction mixture. It was allowed to stir at room temperature for 12 h under nitrogen. The progress if reaction was monitored with TLC. After completion of reaction, excess of water was added. The solid thus precipitated was filtered and washed with methanol. The obtained crude product was purified by silica gel column chromatography eluting with 5% ethyl acetate: hexane to afford as light yellow solid **4** (180 mg, 65%). ^{1}H NMR (500 MHz, $CDCl_3$): $\delta = 8.27$ (br, 1H), 7.26–7.25 (m, 2H), 7.10–7.07 (m, 9H), 7.02–6.99 (m, 6H), 6.96–6.95 (d, $J = 8.6$ Hz, 2H), 4.99 (br, 1H), 4.25 (br, 1H), 1.44 (s, 9H), 1.40–1.38 ppm (d, $J = 7.1$ Hz, 3H). ^{13}C NMR (100 MHz, $CDCl_3$): $\delta = 170.42$, 155.94, 143.69, 140.77, 140.23, 139.71, 136.02, 131.95, 131.26, 126.31, 118.87, 80.67, 77.37, 50.72, 28.27, 17.54 ppm. IR (KBr): $\tilde{\nu} = 3318$, 3051, 2976, 2927, 1673, 1598, 1520, 1460, 1399, 1366, 1313, 1246, 1162, 1068, 752, 697 cm^{-1}. ESI-MS (*m/z* %): 519 $[M+H]^+$ HRMS: calculated for $C_{34}H_{35}N_2O_3Na = 541.2461$, found $[M+Na]^+ = 541.2450$.

Synthesis of Compound 5

The synthesis of compound **5** (yield:164 mg, 59%) was achieved by following the procedure adopted for the synthesis of compound **4**. ^{1}H NMR (500 MHz, $CDCl_3$): $\delta = 8.27$ (br, 1H), 7.26–7.26 (m, 2H), 7.10–7.07 (m, 9H), 7.02–6.99 (m, 6H), 6.96–6.95 (d, $J = 8.6$ Hz, 2H), 4.99 (br, 1H), 4.25 (br, 1H), 1.44 (s, 9H), 1.40–1.38 ppm (d, $J = 7.1$ Hz, 3H). ^{13}C NMR (100 MHz, $CDCl_3$): $\delta = 170.56$, 155.99, 143.69, 140.77, 140.23, 139.71, 136.02, 131.95, 131.26, 126.31, 118.87, 80.67, 77.37, 50.72, 28.27, 17.54 ppm. IR (KBr): $\tilde{\nu} = 3417$, 3052, 1740, 1674,1603, 1528, 1439, 1404, 1378, 1318, 1218, 1110, 1056, 752, 698 cm^{-1}. ESI-MS (*m/z* %):519 $[M+H]^+$ HRMS: calculated for $C_{34}H_{35}N_2O_3 = 519.2642$, found $[M+H]^+ = 519.2639$.

Synthesis of compound L-Ala-TPE

In 2 mL of dry DCM take a 100 mg of compound **4** add 2 mL of TFA at 0 °C, the resulting mixture was stirred for 4 h. The progress of reaction was monitored by TLC. After completion of reaction, the solvent was removed under vacuum afforded compound **L-Ala-TPE** as pale yellow solid (60 mg, 75%). ^{1}H NMR (300 MHz, DMSO-d_6): $\delta = 10.35$ (s, 1H), 8.15 (s, 1H), 7.38–7.35 (d, $J = 8.4$ Hz, 2H), 7.17–7.12, (m, 9H), 7.01–6.93 (m, 8H), 3.94 (s,1H), 1.44–1.41 ppm (d, $J = 7.0$ Hz, 3H). ^{13}C NMR (75 MHz, DMSO-d_6): $\delta =$ 168.06, 143.01, 140.33, 139.92, 138.78, 136.36, 131.56, 131.16, 127.79, 126.50, 126.42. 118.61, 48.94, 17.07 ppm; IR (KBr): $\tilde{\nu} = 3426$, 3260, 3054, 2926, 1675, 1602, 1539, 1510, 1441, 1308, 1249, 1204, 1138, 840, 749, 698 cm^{-1}. ESI-MS (*m/z* %): 419 $[M+H]^+$; HRMS: calculated for $C_{34}H_{35}N_2O_3 = 419.2117$, found $[M+H]^+ = 419.2109$.

Synthesis of compound D-Ala-TPE

For the synthesis of ***D-Ala-TPE*** (yield: 62 mg, 77%), the same experimental procedure described for the preparation of ***L-Ala-TPE*** was employed. ^{1}H NMR (300 MHz, DMSO-d_6): $\delta = 10.33$ (s, 1H), 8.14 (s, 1H), 7.37–7.34 (d, $J = 8.4$ Hz, 2H), 7.16–7.11, (m, 9H), 7.00–6.92 (m, 8H), 3.92 (s,1H), 1.42–1.40 ppm (d, $J = 7.0$ Hz, 3H); ^{13}C NMR (75 MHz, DMSO-d_6): $\delta = 167.95$, 142.88, 140.34, 140.12, 136.32, 131.56, 131.17, 127.71, 126.42. 118.61, 48.92, 19.99 ppm; ESI-MS (*m/z* %): 419 $[M+H]^+$; HRMS: calculated for $C_{34}H_{35}N_2O_3 = 419.2117$, found $[M+H]^+ = 419.2109$.

Synthesis of target molecules

Synthesis of compound NDI-(L-Ala-TPE)$_2$

1,4,5,8 Naphthalene tetracarboxylic dianhydride (50 mg, 0.18 mmol) and compound **L-Ala-TPE** (192 mg, 0.46 mmol) were suspended in 10 mL dry DMF. To this solution Et_3N (0.1 mL) was added and allowed to heat at 120 °C for 15 h. The completion of reaction was monitored by TLC. After completion of reaction, the reaction mixture was cooled to room temperature, and then added excess of water. The precipitated solid was filtered and washed with methanol. The obtained crude product was purified by silica gel column chromatography eluting with 20% ethyl acetate: hexane to afford compound **NDI-(L-Ala-TPE)$_2$** as light yellow solid (120 mg, 60%). Polarimetric measurements: $[\alpha]_{589}^{25} = -55.50$ ($c = 3.1$ mg mL^{-1} in $CHCl_3$); M.P. 342–345 °C; ^{1}H NMR (400 MHz, $CDCl_3$): $\delta = 8.73$ (s, 4H), 7.47 (br, 2H), 7.27 (m, 4H), 7.09–6.96 (m, 34H), 5.84–5.79 (q, 2H), 1.84–1.82 ppm (d, $J = 7.0$ Hz, 6H). ^{13}C NMR (100 MHz, $CDCl_3$): $\delta = 166.98$, 162.48, 143.65, 140.24, 135.49, 132.00, 131.27, 126.46, 119.37, 51.33, 29.68, 14.77 ppm. IR (KBr): $\tilde{\nu} = 3385$, 3077, 2929, 1708, 1669, 1588, 1524, 1524, 1449, 1373, 1250, 769, 696 cm^{-1}. MALDI-TOF: calculated for $C_{72}H_{52}N_4O_6$ 1068.23 found $[M]^+ = 1068.24$.

Synthesis of compound NDI-(D-Ala-TPE)$_2$

The compound **NDI-(D-Ala-TPE)$_2$** (yield:116 mg, 58%) was synthesized by following the procedure adopted for the synthesis of compound **NDI-(L-Ala-TPE)$_2$**. Polarimetric measurements: $[\alpha]_{589}^{25} = +$ 64.20 ($c = 3.1$ mg mL^{-1} in $CHCl_3$); M.P. 342–345 °C; ^{1}H NMR (400 MHz, $CDCl_3$): $\delta = 8.74$ (s, 4H), 7.45 (br, 2H), 7.27–7.25 (m, 4H), 7.11–6.96 (m, 34H), 5.85–5.80 (q, 2H), 1.84–1.83 ppm (d, $J = 7.0$ Hz, 6H). ^{13}C NMR (100 MHz, $CDCl_3$): $\delta = 166.98$, 162.48, 143.65, 140.24, 135.49, 132.00, 131.27, 126.46, 119.37, 51.33, 29.68, 14.77 ppm. IR (KBr): $\tilde{\nu} = 3380$, 3077, 2925, 1708, 1669, 1588, 1524, 1524, 1449, 1373, 1250, 769, 696 cm^{-1}. MALDI-TOF: calculated for $C_{72}H_{52}N_4O_6$ 1068.23 found $[M]^+ = 1068.57$.

Acknowledgements

S.V.B. (IICT) is grateful for financial support from the SERB (DST) SB/S1/IC-009/2014, New Delhi, India and IICT/Pubs./2018/122. S.V.B. (GU) acknowledges financial support and Professorship from the UGC-FRP.

Conflict of interest

The authors declare no conflict of interest.

Keywords: aggregation-induced emission · chiral supramolecular · naphthalene diimide (NDI) · self-assembly · tetraphenylethylene

[1] a) J. Luo, Z. Xie, J. W. Y. Lam, L. Cheng, H. Chen, C. Qiu, H. S. Kwok, X. Zhan, Y. Liu, D. Zhu, B. Z. Tang, *Chem. Commun.* **2001**, 1740 – 1741; b) Y. Hong, J. W. Y. Lam, B. Z. Tang, *Chem. Soc. Rev.* **2011**, *40*, 5361 – 5388; c) J. Mei, N. L. C. Leung, R. T. K. Kwok, J. W. Y. Lam, B. Z. Tang, *Chem. Rev.* **2015**, *115*, 11718 – 11940.

[2] a) D. D. La, S. V. Bhosale, L. A. Jones, S. V. Bhosale, *ACS Appl. Mater. Interfaces* **2018**, *10*, 12189 – 12216; b) A. N. Ramya, M. M. Joseph, J. B. Nair, V. Karunakaran, N. Narayanan, K. K. Maiti, *ACS Appl. Mater. Interfaces* **2016**, *8*, 10220 – 10225; c) J. Mei, Y. Huang, H. Tian, *ACS Appl. Mater. Interfaces* **2018**, *10*, 12217 – 12261; d) X. Lou, Y. Hong, S. Chen, C. W. T. Leung, N. Zhao, B. Situ, J. W. Y. Lam, B. Z. Tang, *Sci. Rep.* **2014**, *4*, 4272; e) C. Orofino, C. Foucher, F. Farrell, N. J. Findlay, B. Breig, A. L. Kanibolotsky, B. Guilhabert, F. Vilela, N. Laurand, M. D. Dawson, P. J. Skabara, *J. Polym. Sci. Part A* **2017**, *55*, 734 – 746; f) K.-H. Ong, B. Liu, *Molecules* **2017**, *22*, 897; g) F. Wu, Y. Shan, X. Li, Q. Song, L. Zhu, *Org. Electron.* **2016**, *39*, 323 – 327; h) A. Rananaware, A. Gupta, J. Li, A. Bilic, L. Jones, S. Bhargava, S. V. Bhosale, *Chem. Commun.* **2016**, *52*, 8522 – 8525.

[3] a) M. Salimimarand, D. D. La, S. V. Bhosale, L. A. Jones, S. V. Bhosale, *Appl. Sci.* **2017**, *7*, 1119; b) W. Zheng, G. Yang, S.-T. Jiang, N. Shao, G.-Q. Yin, L. Xu, X. Li, G. Chen, H.-B. Yang, *Mater. Chem. Front.* **2017**, *1*, 1823 – 1828; c) H.-T. Feng, S. Song, Y.-C. Chen, C.-H. Shen, Y.-S. Zheng, *J. Mater. Chem. C* **2014**, *2*, 2353 – 2359; d) T. Zhang, G.-L. Zhang, Q.-Q. Yan, L.-P. Zhou, L.-X. Cai, X.-Q. Guo, Q.-F. Sun, *Inorg. Chem.* **2018**, *57*, 3596 – 3601; e) N. B. Shustova, T.-C. Ong, A. F. Cozzolino, V. K. Michaelis, R. G. Griffin, M. Dincă, *J. Am. Chem. Soc.* **2012**, *134*, 15061 – 15070; f) J. Huang, Y. Yu, L. Wang, X. Wang, Z. Gu, S. Zhang, *ACS Appl. Mater. Interfaces* **2017**, *9*, 29030 – 29037; g) M. Salimimarand, D. D. La, M. A. Kobaisi, S. V. Bhosale, *Sci. Rep.* **2017**, *7*, 42898; h) S. Song, Y.-S. Zheng, *Org. Lett.* **2013**, *15*, 820 – 823.

[4] a) H. Li, J. Cheng, H. Deng, E. Zhao, B. Shen, J. W. Y. Lam, K. S. Wong, H. Wu, B. S. Li, B. Z. Tang, *J. Mater. Chem. C* **2015**, *3*, 2399 – 2404; b) N.-N. Liu, S. Song, D.-M. Li, Y.-S. Zheng, *Chem. Commun.* **2012**, *48*, 4908 – 4910; c) C. Liu, G. Yang, Y. Si, X. Pan, *J. Phys. Chem. C* **2018**, *122*, 5032 – 5039; d) F. Meng, Y. Sheng, F. Li, C. Zhu, Y. Quan, Y. Cheng, *RSC Adv.* **2017**, *7*, 15851 – 15856; e) H. Li, X. Zheng, H. Su, J. W. Y. Lam, K. Sing Wong, S. Xue, X. Huang, X. Huang, B. S. Li, B. Z. Tang, *Sci. Rep.* **2016**, *6*, 19277.

[5] Anuradha, D. D. La, M. Al Kobaisi, S. V. Bhosale, *Sci. Rep.* **2015**, *5*, 15652.

[6] Anuradha, D. D. La, M. Al Kobaisi, A. Gupta, S. V. Bhosale, *Chem. Eur. J.* **2017**, *23*, 3950 – 3956.

[7] M. Al Kobaisi, S. V. Bhosale, K. Latham, A. M. Raynor, S. V. Bhosale, *Chem. Rev.* **2016**, *116*, 11685 – 11796.

[8] a) Y. Hu, Y. Qin, X. Gao, F. Zhang, C.-A. Di, Z. Zhao, H. Li, D. Zhu, *Org. Lett.* **2012**, *14*, 292 – 295; b) S. V. Bhosale, C. H. Jani, S. J. Langford, *Chem. Soc. Rev.* **2008**, *37*, 331 – 342; c) N. Sakai, J. Mareda, E. Vauthey, S. Matile, *Chem. Commun.* **2010**, *46*, 4225 – 4237; d) S. V. Bhosale, S. V. Bhosale, S. K. Bhargava, *Org. Biomol. Chem.* **2012**, *10*, 6455 – 6468.

[9] a) J. F. Martinez, N. T. La Porte, M. R. Wasielewski, *J. Phys. Chem. C* **2018**, *122*, 2608 – 2617; b) J. Chang, Q. Ye, K.-W. Huang, J. Zhang, Z.-K. Chen, J. Wu, C. Chi, *Org. Lett.* **2012**, *14*, 2964 – 2967; c) A. Das, S. Ghosh, *Chem. Commun.* **2016**, *52*, 6860 – 6872; d) P. Pengo, G. D. Pantoş, S. Otto, J. K. M. Sanders, *J. Org. Chem.* **2006**, *71*, 7063 – 7066; e) D. Shukla, S. F. Nelson, D. C. Freeman, M. Rajeswaran, W. G. Ahearn, D. M. Meyer, J. T. Carey, *Chem. Mater.* **2008**, *20*, 7486 – 7491.

[10] a) A. Rananaware, D. D. La, S. V. Bhosale, *RSC Adv.* **2015**, *5*, 56270 – 56273; b) A. Rananaware, D. D. La, S. M. Jackson, S. V. Bhosale, *RSC Adv.* **2016**, *6*, 16250 – 16255.

[11] T.-T. Wei, J. Zhang, G.-J. Mao, X.-B. Zhang, Z.-J. Ran, W. Tan, R. Yu, *Anal. Methods* **2013**, *5*, 3909 – 3914.

[12] a) A. Jain, S. J. George, *Mater. Today* **2015**, *18*, 206 – 214; b) J. Kang, D. Miyajima, T. Mori, Y. Inoue, Y. Itoh, T. Aida, *Science* **2015**, *347*, 646 – 651; c) F. J. M. Hoeben, P. Jonkheijm, E. W. Meijer, A. P. H. J. Schenning, *Chem. Rev.* **2005**, *105*, 1491 – 1546; d) S. S. Babu, V. K. Praveen, A. Ajayaghosh, *Chem. Rev.* **2014**, *114*, 1973 – 2129; e) J.-M. Lehn, *Angew. Chem. Int. Ed.* **2013**, *52*, 2836 – 2850; *Angew. Chem.* **2013**, *125*, 2906 – 2921; f) Z. M. Hudson, D. J. Lunn, M. A. Winnik, I. Manners, *Nat. Commun.* **2014**, *5*, 3372.

[13] a) C. C. Lee, C. Grenier, E. W. Meijer, A. P. H. J. Schenning, *Chem. Soc. Rev.* **2009**, *38*, 671 – 683; b) M. Yang, N. A. Kotov, *J. Mater. Chem.* **2011**, *21*, 6775 – 6792; c) M. Yamauchi, T. Ohba, T. Karatsu, S. Yagai, *Nat. Commun.* **2015**, *6*, 8936; d) E. Yashima, N. Ousaka, D. Taura, K. Shimomura, T. Ikai, K. Maeda, *Chem. Rev.* **2016**, *116*, 13752 – 13990.

[14] a) A. Brizard, C. Aimé, T. Labrot, I. Huc, D. Berthier, F. Artzner, B. Desbat, R. Oda, *J. Am. Chem. Soc.* **2007**, *129*, 3754 – 3762; b) C. Kulkarni, K. K. Bejagam, S. P. Senanayak, K. S. Narayan, S. Balasubramanian, S. J. George, *J. Am. Chem. Soc.* **2015**, *137*, 3924 – 3932; c) E. T. Pashuck, S. I. Stupp, *J. Am. Chem. Soc.* **2010**, *132*, 8819 – 8821; d) S. Ahmed, B. Pramanik, K. N. A. Sankar, A. Srivastava, N. Singha, P. Dowari, A. Srivastava, K. Mohanta, A. Debnath, D. Das, *Sci. Rep.* **2017**, *7*, 9485; e) P. J. M. Stals, P. A. Korevaar, M. A. J. Gillissen, T. F. A. de Greef, C. F. C. Fitié, R. P. Sijbesma, A. R. A. Palmans, E. W. Meijer, *Angew. Chem. Int. Ed.* **2012**, *51*, 11297 – 11301; *Angew. Chem.* **2012**, *124*, 11459 – 11463.

[15] Y. J. Wang, Z. Li, J. Tong, X. Y. Shen, A. Qin, J. Z. Sun, B. Z. Tang, *J. Mater. Chem. C* **2015**, *3*, 3559 – 3568.

[16] F. Wang, M. Qin, T. Peng, X. Tang, A. Y. Dang, C. Feng, *Langmuir* **2018**, *34*, 7869 – 7876.

[17] Gaussian 09, Revision A.02, M. J. Frisch, G. W. Trucks, H. B. Schlegel, G. E. Scuseria, M. A. Robb, J. R. Cheeseman, G. Scalmani, V. Barone, G. A. Petersson, H. Nakatsuji, X. Li, M. Caricato, A. Marenich, J. Bloino, B. G. Janesko, R. Gomperts, B. Mennucci, H. P. Hratchian, J. V. Ortiz, A. F. Izmaylov, J. L. Sonnenberg, D. Williams-Young, F. Ding, F. Lipparini, F. Egidi, J. Goings, B. Peng, A. Petrone, T. Henderson, D. Ranasinghe, V. G. Zakrzewski, J. Gao, N. Rega, G. Zheng, W. Liang, M. Hada, M. Ehara, K. Toyota, R. Fukuda, J. Hasegawa, M. Ishida, T. Nakajima, Y. Honda, O. Kitao, H. Nakai, T. Vreven, K. Throssell, J. A. Montgomery, Jr., J. E. Peralta, F. Ogliaro, M. Bearpark, J. J. Heyd, E. Brothers, K. N. Kudin, V. N. Staroverov, T. Keith, R. Kobayashi, J. Normand, K. Raghavachari, A. Rendell, J. C. Burant, S. S. Iyengar, J. Tomasi, M. Cossi, J. M. Millam, M. Klene, C. Adamo, R. Cammi, J. W. Ochterski, R. L. Martin, K. Morokuma, O. Farkas, J. B. Foresman, and D. J. Fox, Gaussian, Inc., Wallingford CT, **2016**.

[18] N. M. O'boyle, A. L. Tenderholt, K. M. Langner, *J. Comput. Chem.* **2008**, *29*, 839 – 845.

Manuscript received: September 24, 2018
Revised manuscript received: November 1, 2018
Accepted manuscript online: November 12, 2018
Version of record online: November 26, 2018